

Evaluating the efficiency of payload delivery by ADCs using a minimal PBPK model

ACoP6 2015

Poster ID: S-04/M-26



Linzhong Li, Rachel Rose, Krishna Machavaram, Iain Gardner, Masoud Jamei.

Simcyp (Certara), Sheffield, UK. Correspondence: linzhong.li@certara.com



OBJECTIVES Antibody drug conjugates (ADCs) aim to deliver a sufficient amount of payload (cytotoxic drug) into tumor cells whilst minimizing exposure of healthy tissues to the free payload. The amount of payload internalized into tumor cells depends on a number of factors including target antigen level, ADC internalization rate, target binding affinity, de-conjugation rate and extent of off-target binding, etc.. An integrated approach is needed to model the interplay of these multiple factors. For this purpose a minimal PBPK model for ADCs coupled with a full PBPK model for released payload was used to describe the disposition of ADCs *in vivo* and to evaluate the efficiency of payload delivery to a solid tumor.

METHODS A minimal PBPK model for monoclonal antibodies (mAb) [1] was adapted to describe each ADC species (defined by payload: mAb ratio, i.e., DAR) with payload release [2] leading to inter-conversion between ADC species (figure 1). A tumor model with the same structure as that for tissue was added into the PBPK framework, this is an extension of the solid tumor model developed by Thurber et al [3]. For solid tumor, in contrast to normal tissue diffusion rather than convection is the dominant mechanism for transport of ADC species across the blood vessel wall. The diffusion process is mainly characterized by the average radius of tumor tissue surrounding each blood vessel R_{krogh} , representing the density of tumor blood vessels [3]. Full, quasi-steady state, and Michaelis-Menten models for target-mediated drug disposition (TMDD) were extended to allow multiple ADC species to compete for binding to a single target, with the additional possibility that target binding can occur at multiple sites. Mass fluxes from all possible routes of drug release (including non-specific catabolism in tissue and plasma, de-conjugation in plasma and tissue, and specific catabolism via target binding and subsequent internalization) were tracked and summated. These fluxes are fed into the full PBPK model for small molecule drugs, see Figure 2.

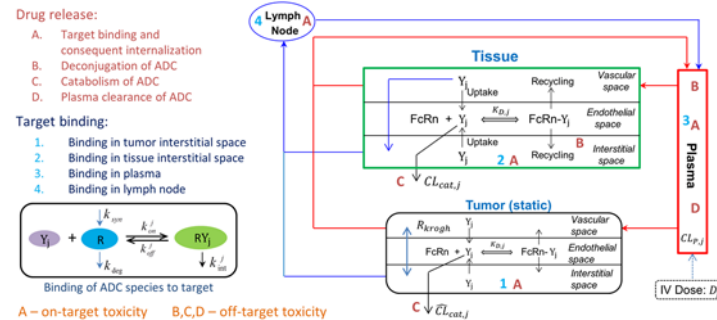


Figure 1 A schematic representation of a minimal PBPK model for ADCs. Y_j -- ADC species with DAR j . The model encompasses (1) an additional tumor compartment, (2) binding of ADC species and target at multiple sites, (3) tracking of mass fluxes of released payload from different routes of release, which can be incomplete and delayed [2], so that (4) released payload can be mechanistically related to either on-target or off-target toxicity.

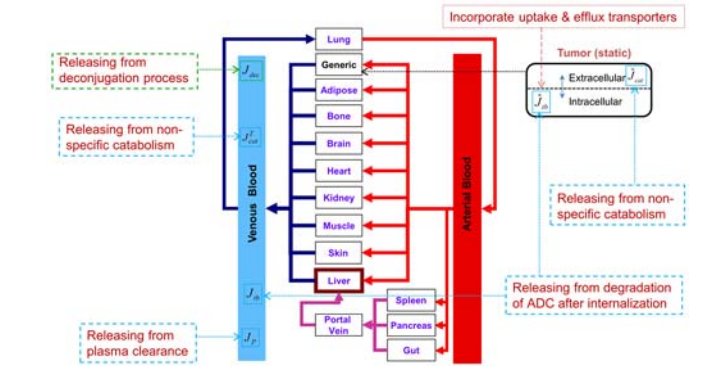


Figure 2 Mass fluxes generated from different routes of payload release are fed into a full PBPK model for small molecule drugs. The model includes a tumor compartment with the action of both uptake and efflux drug transporters accounted for.

Validation of the tumor model was done using tumor uptake data for the huA33 antibody [5] by setting $DAR=0$ in the model and by varying antigen levels and R_{krogh} in realistic ranges. The clinical data obtained by PET imaging [6] were well recovered (results not shown).

The efficiency of payload delivery by ADCs to a solid tumor can be evaluated by defining the percentage of injected payload being internalized into tumor cells, as shown below.

$$\%ID(t) = \frac{\int_0^t D_{int}^{tumor}(\tau) d\tau}{\sum_{j=1}^J \int_0^t C_j(\tau) d\tau} \cdot 100\% = \frac{\text{Accumulated amount up to time } t \text{ of the internalized payload in tumor}}{\text{Amount of payload being administrated into plasma}} \cdot 100\%$$

RESULTS Figure 3 shows typical outputs from the model. The kinetics of the payload show typical formation-limited metabolite profile. Rates of declining conjugated Ab, conjugated drug, and released payload are converging as time progresses, see figure 3B. In addition, the model shows a good sensitivity of the averaged DAR profile on deconjugation rates (k_{dec}), see Figure 3D.

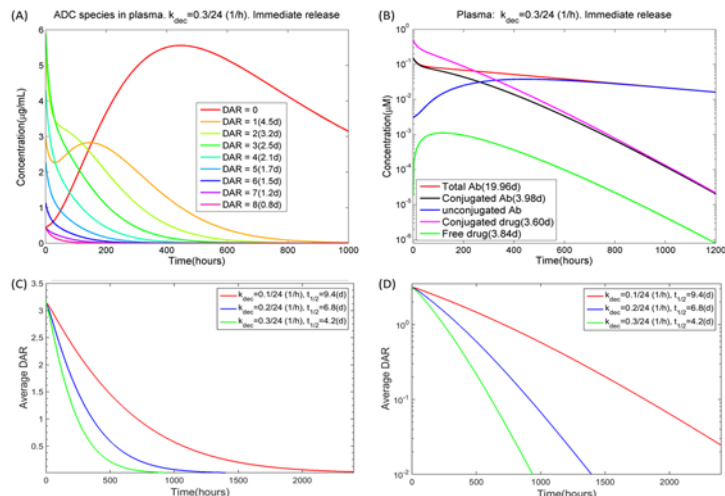


Figure 3 Typical ADC profiles generated by the ADC model for IV dose of $D = 1 \text{ mg/kg}$ with initial DAR distribution: $D_j = f_j D$, $j = 1, \dots, 8$, $f_0 = 0.02$, $f_1 = 0.13$, $f_2 = 0.23$, $f_3 = 0.26$, $f_4 = 0.19$, $f_5 = 0.10$, $f_6 = 0.05$, $f_7 = 0.02$, $f_8 = 0.02$ (data from Bender's paper [4]). The simulation was done without target binding and deconjugation rate was set as $k_{dec} = k_{dec}[1 + (j-1)\theta]$, $\theta = 0.315$ [2]. (A) concentration profiles of individual ADC DAR species. (B) plasma total Ab, conjugated Ab, unconjugated Ab, conjugated drug, and released drug and their half-life are presented. (C)&(D) Average DAR profiles (on linear and log scale) in plasma defined by $DAR_{average}(t) = 2 \sum_{j=1}^J C_j^2(t) / \sum_{j=1}^J C_j(t)$.

One general issue in target selection for ADC drugs is whether more efficient payload delivery would be achieved with an antigen that has high expression and a low internalization rate or with an antigen that has low expression and a high internalization rate. To address this issue some simulations were performed.

The impact of antigen level in normal tissue on %ID in the tumor was first simulated, see Figure 4A.

- The time for %ID to reach steady-state (i.e. the maximal percentage of payload delivery achievable) varied with the tissue to tumor antigen ratio
- The level of the maximal %ID is dose-proportional and depends on R_{krogh} (see figure 4B) due to diffusion-limited delivery of ADCs to tumor.
- The maximal %ID is achievable with a range of antigen levels and internalization rate combinations at different doses (figure 5A) and with varying the ADC affinity to antigen (figure 5B).
- If conjugation decreases binding to FcRn or to target this can result in a reduction in %ID, i.e., efficiency of payload delivery into tumor cells (Figure 6)

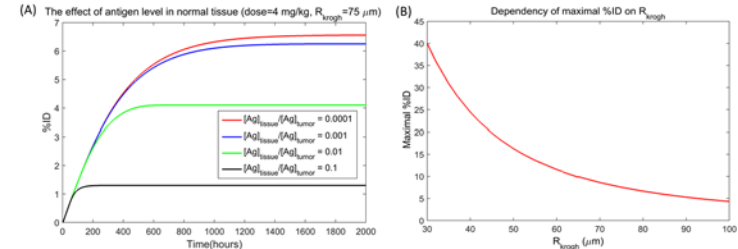


Figure 4 The simulation is based on the initial DAR distribution and deconjugation rates with $k_{dec} = 0.1/24$ (1/h) used in Figure 3. $k_{on} = 2520$ ($\mu\text{M h}^{-1}$), $k_{off} = 1.26$ (h^{-1}) ($K_D^j = 0.5 \text{ nM}$), $K_{D,FCRn} = 0.728 \mu\text{M}$, $k_{int} = k_{deg} = 0.1$ (1/h), $j=0, \dots, 8$ for both tissue and tumor. Tumor antigen level is fixed as $[Ag]_{tumor} = 0.2 \mu\text{M}$.

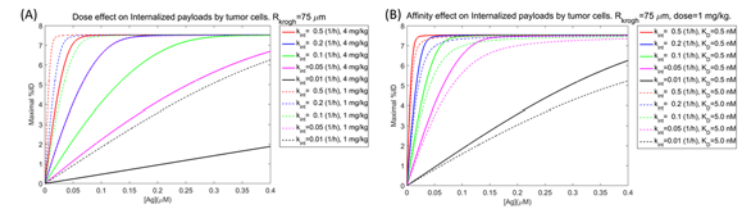


Figure 5 Simulations of maximal %ID for a range of antigen level [0, 0.4 μM] and varying internalization rate constant $k_{int} = 0.01, 0.05, 0.1, 0.2, 0.5$ (1/h). (A) two different doses; (B) two different binding affinities.

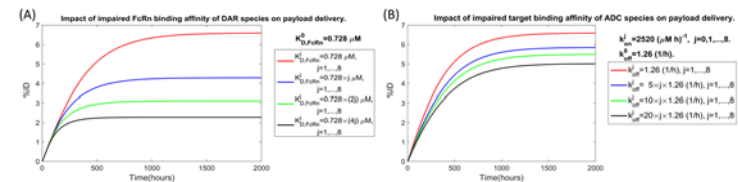


Figure 6 In this simulation tumor antigen level is fixed to 0.2 μM , and $k_{int} = k_{deg} = 0.1$ (1/h), $j=0, \dots, 8$. (A) Impaired binding affinity to FcRn; (B) Impaired binding affinity to antigen.

CONCLUSION A minimal PBPK model is developed for ADCs, which also incorporates a mechanistic tumor model to allow the study of payload delivery to the tumor. The percentage of injected drug (payload) being internalized into tumor cells was used to assess the efficiency of payload delivery. In this simulation study, it is shown that a high efficiency of payload delivery can be achieved by either a high level of antigen with a low internalization rate or a low level of antigen with a high internalization rate, but was also dependent on several other factors, such as dose, binding affinities to target and FcRn, and the density of tumor blood vessels. This complex interplay of multiple factors exemplifies the need for an integrated modelling and simulation approach to understand the disposition of ADCs.

REFERENCES

1. Li, L., et al., *Simulation of monoclonal antibody pharmacokinetics in humans using a minimal physiologically based model*. AAPS J, 2014. 16(5): p. 1097-109.
2. Gibiansky, L. and E. Gibiansky, *Target-mediated drug disposition model and its approximations for antibody-drug conjugates*. J Pharmacokinetic Pharmacodyn, 2014. 41(1): p. 35-47.
3. Thurber, G.M. and K. Dane Wittup, *A mechanistic compartmental model for total antibody uptake in tumors*. J Theor Biol, 2012. 314: p. 57-68.
4. Bender, B., et al., *A mechanistic pharmacokinetic model elucidating the disposition of trastuzumab emtansine (T-DM1), an antibody-drug conjugate (ADC) for treatment of metastatic breast cancer*. AAPS J, 2014. 16(5): p. 994-1008.
5. Ackerman, M.E., et al., *A33 antigen displays persistent surface expression*. Cancer Immunol Immunother. 2008. 57(7): 1017-1027.
6. Carrasquillo, J.A., et al., *124I-huA33 Antibody PET of Colorectal Cancer*. 2011. 52: 1173-1180.
7. Chen, Y., et al., *Physiologically based pharmacokinetic modeling as a tool to predict drug interactions for antibody drug conjugates*. Clin Pharmacokinetic. 2015. 54(1): 81-93.